Migration Law of Suspended Nano Zero Valent Iron in Rough Single Fractures

Rong Wu

373961084@qq.com

School of Civil Engineering, Wanjiang University of Technology, maanshan 243031, China

Abstract. Water flow and solute transport experiments in fractured rock mass systems can provide effective theoretical support and experimental model research basis for many fields, such as deep groundwater pollutant transport, remediation agent injection technology in the process of pollutant treatment. This article uses artificial horizontal rough fractures and natural rock materials as indoor physical experimental models to study the migration of suspended nZVI in artificial horizontal rough fractures and natural rock horizontal rough single fractures. The migration simulation results in the two fractures are compared, and the migration characteristics of nZVI in rough single fractures are proposed.

Keywords: rough single fractures; nano zero valent iron; solute transport

1 Introduction

With the development of society, environmental issues have become increasingly urgent, and how to solve the migration of pollutants in water has always been a concern (Lefevre E, Bossa 2016, Mukherjee, Kumar, 2016, Yirsaw, Megharaj 2016)[1][2][3]. In addition, it is particularly important to successfully apply pollutant remediation agents to the pollution sources that need to be treated. In recent years, many fundamental experimental works have been conducted both domestically and internationally on water flow and solute transport in ideal single fractures. The problem of solute transport in rock fractures has always been a concern, and water flow tests and tracer tests are often used as the basis for development. In recent years, with the continuous deepening of research on solute transport in rock fractures, different scholars have conducted different flow rates or concentrations of solute transport experiments in real fractured rock masses. Some volatile groundwater pollutants and the migration patterns of pollutant remediation agents are receiving increasing attention from experts.

Nano scale Zero Valent Iron (nZVI) is an iron particle with a particle size between 1-100 nanometers (Cohen and Weisbrod 2018)[4][5]. Its specific surface area can reach 10-70 m^2/g, which is dozens of times the specific surface area of ordinary iron powder and iron filings, making nZVI have stronger chemical reaction activity. The electrode potential of zero valent iron is E0 (Fe^{2+}/Fe^0)=-0.44V, which is easily oxidized and releases electrons in the environment. This strong reducibility is widely used in groundwater pollution control. NZVI can not only degrade haloalkane in groundwater pollutants, but also some organic pollutants without halogens. At the same time, it can eliminate heavy metal ions and various inorganic anions in groundwater. In the past decade, the application of nZVI in groundwater pollution

IDEE 2023, November 24-26, Zhengzhou, People's Republic of China

DOI 10.4108/eai.24-11-2023.2343447

remediation technology has received widespread attention from relevant research institutions both domestically and internationally (Mueller, Braun et al. 2012, Zafar, Javed, et al. 2021,Plessl K, Russ A, et al. 2023)[6][7][8].

NZVI particles have strong magnetic cohesion and are easy to aggregate into iron particles with micron size, resulting in a decrease in their specific surface area and thus reducing the degradation rate of pollutants (Cohen and Weisbrod 2018, Mondino, Piscitello, et al. 2020)[5][9]. To solve the above problems, it is necessary to perform suspension stability treatment on nZVI. Scientists from various countries have developed many methods to achieve stable suspension and long-distance transport of nZVI in water, and conducted indoor research on the transport of suspended nZVI in two -dimensional porous media, revealing some important regular phenomena. However, there have been no relevant studies on the transport laws of suspended nZVI solutes in fractured rock mass systems.

Conducting water flow and solute transport experiments in fractured rock mass systems can provide effective theoretical support and experimental model research foundation for many fields, such as deep groundwater pollutant transport and remediation agent injection technology in pollutant treatment processes. Using natural rock materials as indoor physical experimental models can lead to unsatisfactory experimental results due to chemical reactions between mineral components on the surface of rock fractures and suspended nZVI solutes; In addition, the wetting angle of the rock surface is relatively large and there are many small pores, so water flow on its surface will also be subject to significant resistance (Lv, Xue et al., 2014)[10].

This article studies the migration experiments of suspended nZVI in artificial horizontal rough fractures and natural rock horizontal rough single fractures, and compares the migration simulation results of the two rough fractures, proposing the migration characteristics of nZVI in rough single fractures.

2 Preparation Of Crushed Rock Blocks

2.1 Production Of Simulated Glass Cracks

The production process includes: 1) selecting liquid gypsum material and pouring the crack surface into a mold; 2) Wait for the gypsum liquid to naturally air dry at room temperature, and slowly and completely peel off the gypsum from the rock; 3) Slowly inject the high-temperature melted liquid glass into the gypsum mold, and the injection process should be carried out slowly to avoid the generation of bubbles; 4) Waiting for the natural air drying of liquid glass at room temperature, the gypsum was peeled off to obtain a complete artificial glass crack similar to the original rock fracture surface.

2.2 Fracturing Treatment of Natural Rocks

The processing process is as follows: 1) Take natural rock mass and cut it into rectangular standard rock blocks; 2) Grind a groove 0.01 m wide and 0.01 m deep around the rock block; 3) Place the rock block in the press, fix it with steel plate and hard foam, and contact the press with diamond shaped metal bar on the top. The standard rock block forms a nearly straight

fracture surface during the pressure application process of the press; 4) Separate the rock block along the fracture surface and clean the surface of the rock block.

Two dolomite sample rock blocks are approximately 350-400mm long, 250-300mm wide, and 90mm thick. The rock sample contains sutured rock surfaces parallel to the dolomite layer. Use a desktop diamond saw blade to cut the sample into 300mm×230mm×70 mm rock block. Cut 5 on the short end and along a long edge of the protruding suture rock surface × A 5mm incision is made using a uniaxial compression loading machine to apply compression load on two 12mm diameter steel rods along the top and bottom notches at both ends, forcing the steel rods into the rock block's notch and inducing fracture. Use a diamond saw blade to remove excess rock from the rock block. The final size of the rock block is approximately 280×210 × 70 mm. The four sides of the rock block are polished using a surface grinder to ensure proper sealing in the stainless steel fracture rock block retention groove using rubber gaskets. Figure 1 Artificial rock block induced fracture.

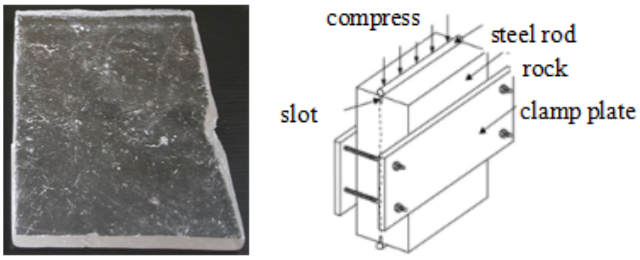

Figure 1 Artificial rock block induced fracture.

3 Test Device and Material

3.1 Test Device

A fully enclosed glass simulation rock mass fracture solute transport system, which can avoid the threat of pollutants to the health and safety of the test personnel, as well as the chemical reaction between rock mineral components and test reagents. It can also visually observe the transport process of colored solutes; The biggest advantage is the fully enclosed experimental system, which is protected by nitrogen gas to avoid contact between the repair agent and air, reduce reagent consumption, avoid the impact of bubbles generated by the oxidation-reduction reaction on the experimental results, and avoid the blockage of solute transport channels by solid precipitates generated by the oxidation-reduction reaction.Figure 2 is a schematic diagram of a laboratory scale fracture rock testing device.

3.2 Material Preparation

The development of reagent preparation and concentration testing methods using carboxy-methyl cellulose (CMC) as a nzVI suspension agent, as well as the testing and acquisition of breakthrough curves for CMC+nzVI solute transport experiments in fractured rock media.

Preparation of CMC carboxymethyl cellulose:(1) soluble in water to form a viscous liquid;(2) White solid powder itself;(3) After being dissolved in water, it can be used as a suspension agent; 4) Prepare CMC solute with a concentration of 3% and stir for 10 hours for later use.

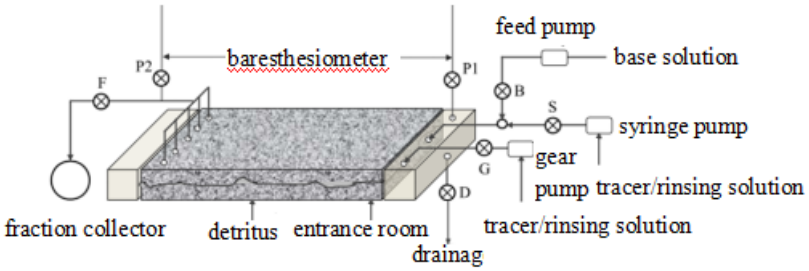

Figure 2 Schematic diagram of the testing device for fractured rock blocks

Preparation of nano zero valent iron (nZVI): (1) Iron particles with a particle size of 10-100 nanometers; (2) Specific surface area 10-70m2/g; (3) Electrode potential -0.44V; 5) Has strong reducibility.

4 Test Plan and Result Analysis

4.1 Hydraulic Test

Perform hydraulic tests on fractured rock blocks to determine the equivalent hydraulic gap width for fracture defined by Tsang (1992)[11] and the specific flow method. Use a multi-channel peristaltic pump to inject water through the fracture to minimize the pulse. Water is discharged from the system through a constant head outlet downstream of the fracture. Use a pressure gauge connected to the upstream inlet chamber and downstream outlet manifold to determine the water head loss at the fracture point. There are five indenters connected to the five outlet needle ports. These five ports are connected together, sometimes there is a difference of approximately 1 to 3.5 millimeters. Take the average value of these water pressure heads as the downstream head. The hydraulic test is conducted at three water flow rates. Determine the equivalent hydraulic gap width (bh) using the following equation:

$$b_h = \sqrt[3]{\frac{12\mu QL}{\Delta HW\gamma}} \qquad (1)$$

Among them, μ is the dynamic viscosity of water (kg. m-1. s-1), Q is the volumetric flow rate of water (m3. s-1), and L is the crack length in the direction of water flow (m); W is the width of the crack in the vertical water flow direction (m), γ is the unit weight of the water (kg.m-2. s-2), and ΔH is the pressure head difference (m) between the upstream and downstream of the crack. For fracture F1, the flow rates for hydraulic tests are 9.00×10-9，1.8×10-8 and 2.70×10-8 m3/s respectively. For fracture F2, the hydraulic test flow rates are 7.67×10-9，1.53×10-8 and 2.30×10-8m3/s respectively. Measure water flow volume by collecting outflow water of known time.

4.2 Solute And Colloid Tracer Transport Test

All solutions were prepared using degassed distillation and buffering (using 1mM NaHCO3) with MilliQ water. The tracer solution was injected into 11 well volumes (PV, calculated based

on equivalent hydraulic gap width), and then 18 PV of tracer free buffer solution was injected. These tests are conducted in 3.5 × 10-4, 7.0 × 10-4 and 1.05 × Conducted under three different specific discharges of 10-3 m/s3. Collect water leaving the fracture system through a distillate collector. The total time for each tracer test (including pulse and flushing) is depending on tracer discharge rate. Standardize the tracer concentration in the effluent section by injecting tracer concentration (C_0) to determine the normalized tracer penetration curve (BTC).

4.3 Design Of Experiments Lgb, Lgb+Cmc, Cmc+Nzvi

(1) The Design of experiments of fracture solute transport adopts two average flow velocities along the fracture direction: 20m/d, 30m/d;

(2) The fracture solute transport tests were conducted using Lissamine Green B (LGB) as the tracer for water flow tests, LGB and Carboxymethyl Cellulose (CMC) as stabilizers for solute transport, and CMC carrying nZVI for suspended nZVI solute transport tests;

(3) During the solute transport experiment in glass cracks, an illuminated light box is installed at the bottom of the crack, and the entire solute transport process is recorded using a high-definition camera. The results are compared with the numerical simulation results;

(4) LGB solute concentration was tested using a UV spectrophotometer at 633nm absorbance peak, CMC concentration was determined using TOC analyzer, nZVI concentration was first fully oxidized after sample acquisition, and 360nm peak UV spectroscopy was used Photometer and Phenanthroline Method testing.

The test was carried out in a single crack glass crack platform, using Carboxymethyl cellulose CMC to carry nZVI for suspended nZVI solute transport test. Reveal the different results of the solute transport experiment when the unit flow rate of water in the crack is different or the concentration of CMC is different. The migration test is characterized by using Lissamine Green B (LGB) to dye the water first, and then using Carboxymethyl cellulose CMC as the stabilizer to carry nano zero valent iron nZVI in an artificial glass crack.

4.4 Image Acquisition of Glass Cracks

4.4.1 Lgb Test

The water flow tracing test was conducted using a unit flow rate of 20m/d and an LGB concentration of 20mg/L. The LGB mass recovery rate was calculated using an ultraviolet spectrophotometer through absorbance calculation, as shown in Figure 3.

4.4.2 Lgb+Cmc Test

The CMC solute transport test was conducted using a unit flow rate of 20m/d, LGB concentration of 20mg/, and CMC concentrations of 0.4% and 0.8%. The LGB mass recovery rate was calculated using an ultraviolet spectrophotometer through absorbance calculation, and the total organic matter concentration was calculated using TOC to obtain the CMC mass recovery rate, as shown in Figure 4.

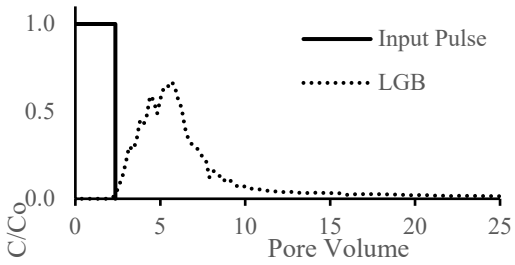

LGB : Specific Discharge (Sp. Dis.) = 20 m/d

Figure 3 LGB Water Flow Tracer Test

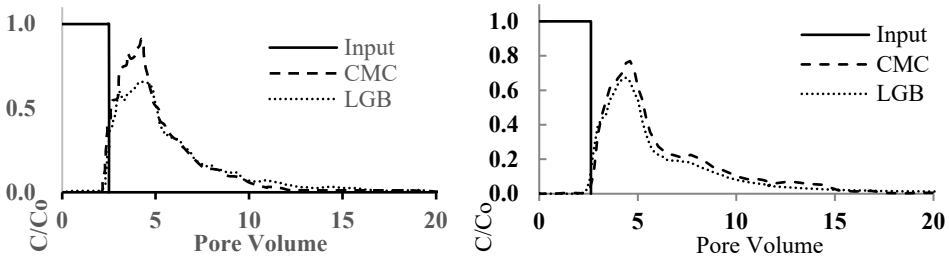

(a) LGB + CMC (0.4%): (b) LGB + CMC (0.8%)

Figure 4 LGB+CMC solute transport test

4.4.3 Nzvi+Cmc Experiment

Using different unit flow rates of 20m/d and 30m/d, and different CMC concentrations of 0.4% and 0.8%, suspension nZVI solute transport experiments were conducted using CMC. After obtaining sufficient oxidation of the sample, the nZVI mass recovery rate was calculated using UV spectrophotometer through absorbance calculation. The total organic matter concentration was calculated using TOC to obtain the CMC mass recovery rate, as shown in Figure 5.

In the CMC suspension nZVI solute transport experiment, the concentration of nZVI prepared by fresh synthesis was 100-2500 mg/L. The stability and characteristics of CMC-nZVI mixture were determined by Transmission electron microscopy, Dynamic light scattering and UV visual spectrophotometry. It can be clearly observed that during the migration process of CMC in cracks, due to the viscous effect, the wake of CMC is higher than that in the LGB tracer experiment. During the water flow test using LGB as a tracer, the wake display varies depending on the unit flow rate. Under the 20m/d condition, it is more pronounced than the 30m/d wake.

The migration process of LGB, CMC, and CMC+nZVI in rock fractures was explored by analyzing the solute concentration of collected samples. Due to adsorption, the peak concentration of nZVI after suspension treatment is much lower than that of CMC and LGB. In the experiment, it was observed that although the cracks were washed with distilled water for 10 hours, a large amount of nZVI remained in the cracks.

In all experiments, the mass recovery rates of LGB and CMC exceeded 90%. However, the higher the injection concentration (0.8%), the higher the peak concentration of CMC. The average lag time between LGB is the shortest, while the average lag time of nZVI is the longest. Due to the influence of liquid viscosity, the migration speed of CMC is relatively small; The migration process of nzVI is influenced by the adsorption effect on the fracture surface. The quality recovery rate of NZVI (50% to 60%) is much lower than that of LGB and CMC.

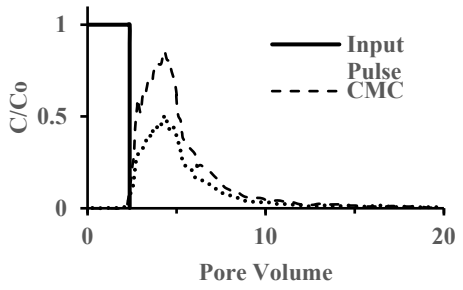

(a)nZVI + CMC (0.4%): Sp. Dis. = 30 m/d

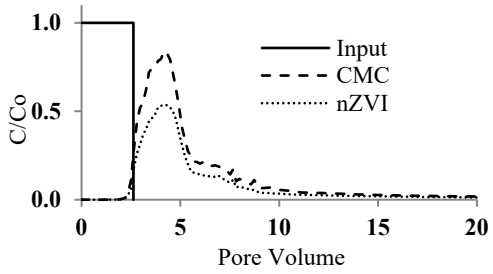

(b)nZVI + CMC (0.8%): Sp. Dis. = 30 m/d

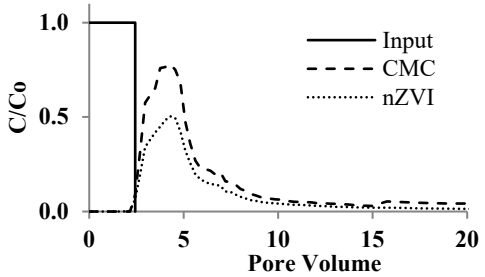

(c)nZVI + CMC (0.8%): Sp. Dis. = 20 m/d

Figure 5 LGB+nZVI solute transport test

4.4.4 Rock Fracture Experiment

Perform the same LGB water flow tracing test, LGB+CMC solute transport test, and CMC suspension nZVI solute transport test in the original template of artificial glass cracks and real

rock mass cracks. Using different unit flow rates of 20m/d and 30m/d, and different CMC concentrations of 0.4% and 0.8%, the samples were fully oxidized. LGB and nZVI mass recovery rates were calculated using UV spectrophotometer through absorbance calculation, and total organic matter concentration was calculated using TOC to obtain CMC mass recovery rates.

5 Conclusion

The mass recovery rate of LGB in rock fractures is lower than that in glass fractures, which is mainly caused by the diffusion of solute into the rock fracture matrix; The mass recovery rate of CMC is relatively high in both glass and rock fractures, mainly due to the weak adsorption of CMC by the two types of fractures and the weak diffusion of solutes in the matrix; CMC changes the hydraulic properties of fractures and creates favorable flow conditions for flushing water, thereby increasing the pollution plume during LGB migration; The quality recovery rate of NZVI is very low, mainly due to the adsorption effect on the crack surface, the pores on the crack surface, the water gas interface, and the working effect of bubbles; The higher the unit discharge, the higher the mass recovery rate and breakthrough curve peak concentration of nZVI and LGB.

Acknowledgments: This work was supported by the Natural Research Science Institute of Universities in Anhui Province (No.KJ2019A1280).

References

[1] Lefevre E, Bossa N, et al. (2016) A review of the environmental implications of in situ remediation by nanoscale zero valent iron (nZVI): behavior, transport and impacts on microbial communities. Science of The Total Environment, 565(15): 889-901. https://doi.org/10.1016/j.scitotenv.2016.02.003.

[2] Mukherjee R, Kumar R, et al. (2016) A review on synthesis, characterization, and applications of nano zero valent iron (nZVI) for environmental remediation.Critical Reviews in Environmental Science and Technology, 46(5):443-466. https://doi.org/10.1080/10643389.2015.1103832.

[3] Yirsaw BD, Megharaj M, et al. (2016). Environmental application and ecological significance of nano-zero valent iron. Journal of Environmental Sciences, 44:88-98. https://doi.org/10.1016/j.jes.2015.07.016

[4] Cohen,M., Weisbrod, N., (2018) Field scale mobility and transport manipulation of carbon-supported nanoscale zerovalent iron in fractured media. Environmental science & technology, 52(14): 7849-7858. https://doi.org/10.1021/acs.est.8b01226.

[5] Cohen,M., Weisbrod, N., (2018) Transport of iron nanoparticles through natural discrete fractures Water research, 129(1): 375-383.https://doi.org/10.1016/j.watres.2017.11.019.

[6] Mueller NC, Braun J, et al. (2012). Application of nanoscale zero valent iron (NZVI) for groundwater remediation in Europe. Environmental Science and Pollution Research, 19:550-558. doi.10.1007/s11356-011-0576-3.

[7] Zafar AM, Javed , et al. (2021) Groundwater remediation using zero-valent iron nanoparticles (nZVI). Groundwater for Sustainable Development, 15:100694. https://doi.org/10.1016/j.gsd.2021.100694

[8] Plessl K, Russ A, et al. (2023) Application and development of zero-valent iron (ZVI) for groundwater and wastewater treatment. International Journal of Environmental Science and Technology , 20:6913-6928. https://doi.org/10.1007/s13762-022-04536-7.
[9] Mondino F, Piscitello A, et al. (2020) Injection of zerovalent iron gels for aquifer nanoremediation: lab experiments and modeling. Water, 12(3):826. https://doi.org/10.3390/w12030826.
[10] Lv X, Xue X, et al. (2014) Nanoscale zero-valent iron (nZVI) assembled on magnetic Fe3O4/graphene for chromium (VI) removal from aqueous solution.Journal of Colloid and Interface Science, 417(1):51-59. https://doi.org/10.1016/j.jcis.2013.11.044.
[11] Tsang YW. (1992)Usage of “equivalent apertures” for rock fractures as derived from hydraulic and tracer tests. Water Resources Research, 28(5):1451–1455. https://doi.org/10.1029%2F92WR00361.